



# Fracture toughness determination methods of WC-Co cemented carbide material at micro-scale from micro-bending method using nanoindentation<sup>☆</sup>

J. Monnet<sup>a</sup>, Y. Gaillard<sup>a</sup>, F. Richard<sup>a</sup>, M. Personeni<sup>b</sup>, S. Thibaud<sup>c,\*</sup>

<sup>a</sup> Université de Franche-Comte, CNRS, Institut FEMTO-ST, Department of Applied Mechanics, Besançon, France

<sup>b</sup> CNRS, Institut FEMTO-ST, Department of Applied Mechanics, Besançon, France

<sup>c</sup> SupMicroTech ENSMM, CNRS, Institut FEMTO-ST, F-25000, Department of Applied Mechanics, Besançon, France

## ARTICLE INFO

Handling editor: M Meyers

### Keywords:

Stress intensity factor  
Micro-scale  
Toughness  
Nanoindentation  
Cemented carbide  
Numerical simulations

## ABSTRACT

Determining toughness properties is crucial for the development of components made of brittle materials, especially at the microscale. Numerous methods rely on establishing a limit load that triggers the propagation of a pre-cracked specimen. The primary challenge lies in accurately and repeatably determining this limit load value. In this study, we introduce a coupled numerical-experimental approach to determine the stress intensity factor at the microscale using a micro-bending test on pre-notched cemented carbide micro-cantilevers. Specimens are fabricated through micro-electrical-discharge milling, and the initial crack is generated using a focused ion beam process to ensure a repeatable crack shape. Geometries are defined to validate beam theories.

Cycling bending tests, employing nanoindentation with three types of loading (fatigue-like, progressive repeated, and ramping sinusoidal loadings), are utilized to ascertain fracture toughness properties of tungsten carbide material at the microscale. Micro-indentation is also conducted conventionally to compare hardness at meso and micro-scales. Analytical methods and finite element analysis are employed to extract the critical stress intensity factor. The cyclic bending test with the proposed ramping sinusoidal loading demonstrates a time shift between the applied force and the displacement, enabling accurate and repeatable detection of the initiation of crack propagation. The primary contributions are associated with the development of a micro-bending test on precracked microcantilevers with ramping sinusoidal loading applied by a nanoindenter device. The miniaturization of specimens and tests, for an equivalent grain size, does not result in a scale effect on toughness properties.

## 1. Introduction

Cemented carbide materials showcase exceptional mechanical, tribological, and thermal properties, making them suitable for various industrial applications, particularly in manufacturing processes such as cutting tools and blanking tools. Their significance is underscored in applications where tribological aspects (wear, friction) and hardness properties are crucial. Notably, cemented carbides possess very high elastic properties, with a Young's modulus value twice as high as that of steel. These unique tribological and material properties are especially appealing for the watchmaking industry.

In watchmaking applications, numerous mechanisms rely on the utilization of compliant parts, such as springs, pawls, and snaps,

necessitating the reduction of energy consumption at interfaces. For instance, Fig. 1 illustrates an indexing system in a mechanical watch, comprising a star wheel indexed by a compliant part known as a jumper. During the indexing between two positions of the star wheel, the jumper undergoes bending. To ensure the system's optimal performance, leading to accurate indexing, it is crucial to store significant elastic energy while minimizing friction and wear at the interfaces. Materials like metallic glasses, ceramics, and carbides are well-suited for such applications, with carbides being particularly relevant from manufacturing and economic perspectives.

The fracture phenomenon is a critical criterion for verifying the integrity of components, especially for brittle materials like ceramics and carbides. To predict the mechanical resistance of components based

<sup>☆</sup> Preprint submitted to Journal of Materials Research and Technology November 27, 2023.

\* Corresponding author. Department of Applied Mechanics, 24 rue de l'épithaphe, F-25000, Besançon, France.

E-mail address: [sebastien.thibaud@ens2m.fr](mailto:sebastien.thibaud@ens2m.fr) (S. Thibaud).

on brittle materials, it is essential to identify toughness properties in correlation with the fracture mode applied to the component, and to determine the associated stress intensity factor.

In fracture mechanics theory, the stress intensity factor  $K$  is employed to predict the stress state in the vicinity of a crack tip. This factor is commonly utilized to establish a failure criterion for brittle materials, assuming linear elastic behavior. The stress intensity factor is defined by the expression:

$$K = \sigma\sqrt{\pi a} f(\alpha) \quad (1)$$

where  $a$  is the initial length of the crack,  $\sigma$  is the magnitude of the far-field applied stress near the crack tip and the  $f$  function is a specimen-dependent function defined from the  $\alpha$ -ratio:

$$\alpha = \frac{a}{w} \quad (2)$$

with  $w$  is the width of the specimen.

From this theory, it is also possible to define three stress intensity factors ( $K_I, K_{II}, K_{III}$ ) associated with three different fracture modes: opening, in-plane shear and out-of-plane shear modes, respectively. In this paper, the study is focused on the determination of the stress intensity factor  $K_I$  in the case of opening mode. In this scenario, it then leads to determining the toughness value by the way of the critical stress intensity factor  $K_C = K_{Ic}$  at fracture.

The precise determination of this property is essential to characterize toughness for a minimum safety coefficient and to avoid overloading products. In fact, the current achievable densities for cemented carbides ( $\rho = 15.6 \text{ g}\cdot\text{cm}^{-3}$ ) are higher than those of conventionally used steels ( $\rho = 7.8 \text{ g}\cdot\text{cm}^{-3}$ ). The study by Ingelstrom and Nordberg [1] experimentally examined the toughness of cemented carbides with a cobalt matrix. The experimental methods includes indentation tests, compact tension (CT) tests, and 3–4 point bending tests. The research revealed a correlation between fracture toughness (FT) and hardness.

In their investigation utilizing 3-point bending tests on cemented carbide (WC-Co), Fang [2] explored the relationship between fracture toughness (FT) and hardness. They demonstrated that the critical stress intensity factor  $K_C$  is dependent on both the cobalt content and mean grain size.

Felten et al. [3] estimated crack growth resistance curves (R-curves) of WC-Co cermet using compact tension (CT) tests. Additionally, they demonstrated the influence of cobalt content and mean grain size on elastic properties (Young's modulus and Poisson's ratio) as well as on the critical stress intensity factor.

Tarragó et al. [4] conducted a study on the influence of the initial microstructure of WC-Co cemented carbide materials on the R-curve behavior. They examined five grades of WC-Co with varying binder content and carbide mean grain size, utilizing 4-point bending fully articulated tests. The investigation clearly demonstrated the impact of these parameters on the values of the critical stress intensity factor.

At the microscale, Bohnert et al. [5] suggested extracting toughness properties through notched micro-cantilever specimen tests on single-crystalline tungsten material. Micro-cantilevers were fabricated using an electrical discharge machining process, and the initial notch was introduced through a focus ion beam (FIB) process. A nano-indentation device was employed to apply a transverse force on the specimen. An inverse method, relying on the correlation between a numerical model and experimental results, was utilized to extract the critical stress intensity factor. The authors also mention that the FIB process used to create the pre-crack does not introduce any defects (nanocracks) at the tip.

Similarly, Pippin et al. [6] conducted a review of characterization techniques for extracting toughness properties at small scales. They also explored the use of the FIB process to create the initial crack geometries on specimens. The latter, being highly repeatable, has no influence on the pre-cracked.

In order to utilize compliant micro-parts in WC-Co, it is crucial to precisely determine the elastic properties and critical stress intensity factors. This paper focuses on defining a method to identify toughness properties of WC-Co cemented carbide material at the micro-scale. As mentioned earlier, in the linear elastic framework, elastic parameters (Young's modulus and Poisson's ratio) are necessary to determine stress intensity factor values. Nanoindentation tests are performed to extract these parameters. A preliminary determination of the critical stress intensity factor at the meso-scale is proposed by using micro-hardness tests (Vickers's tests) to obtain reference measurements, as suggested by Niihara et al. [7], Warren and Matzke [8], Shetty et al. [9], Spiegler et al. [10], and Swab and Wright [11].

The majority of the studies proposed lead to the determination of intensity factors with varying degrees of precision. However, the crucial aspect is initially determining the critical force associated with crack propagation. This determination relies not only on the ability to reproduce the test in terms of sample manufacture and pre-crack (bending tests) or indent (indentation) but also on the test's repeatability. Subsequently, depending on the assumptions and approximations made by analytical or numerical approaches, it becomes possible to trace the value of stress intensity factors. The primary focus of the study proposed in this paper is to define a micro-bending test of pre-cracked micro-cantilevers by applying a time-varying loading. This approach enables the accurate determination of the limit load.

The paper is then focused on the development of a micro-bending test based on micro-cantilever specimens with cyclic loading applied by a nanoindentation device to determine the critical stress intensity factor. For this, three different types of loading are considered to precisely determine the value of the fracture force that initiates crack propagation. This value is obtained accurately and with higher repeatability by observing force/displacement curves and also from the time shifting between the applied force and the nanoindenter displacement during the test in the case of ramping sinusoidal loading. The critical

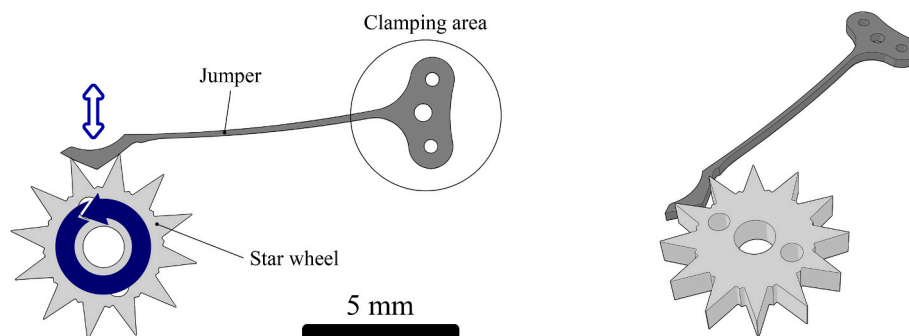


Fig. 1. Indexation system on a mechanical watch movement.

stress intensity factor value is extracted by using the fracture force value as an input parameter of an equivalent finite element model of the micro-bending. Comparisons between the proposed method, micro-hardness tests, and the literature are provided and show a good correlation with the study proposed by Tarragó et al. [4].

## 2. Materials and methods

### 2.1. Material

A WC-Co cemented carbide material is considered and it is based on the combination of two phases:

- A 90 % tungsten carbide (wt%) hard phase that ensures hardness and wear resistance but also leads to a high density value;
- A 10 % cobalt (wt%) matrix binder phase, which is more ductile than the tungsten carbide phase and allows for good resilience.

These two-phase materials are obtained through a hot sintering process (1500 °C), and the composition is widely used in manufacturing processes for cutting tools applications where mechanical, thermal, and tribological behaviors are critical. As mentioned by Okamoto et al. [12], WC grain size is a key parameter to define a brittle or a ductile WC-Co material. In Fig. 2, an Atomic Force Microscopy analysis is presented to determine WC grain size. From this analysis and by using planimetric measurement, an average grain size of  $0.6 \pm 0.1 \mu\text{m}$  is obtained.

This material exhibits a brittle behavior, aligning with the conclusions of Okamoto et al. [12]. The authors demonstrated that brittle behavior is associated with a small grain size of WC, while a ductile mode is obtained for a grain size greater than  $20\mu\text{m}$ . Although some grains were evaluated to be  $1\mu\text{m}$  in size, a limited variability was observed, indicating a homogeneous structure. A surface analysis of the material microstructure confirms the cobalt phase proportion to be close to 10 %, as expected from the initial specification.

### 2.2. Local measurement of Young's modulus by nanoindentation tests

As mentioned earlier, stress intensity factors are directly connected to the elastic properties defined by Young's modulus  $E$  and Poisson's ratio  $\nu$ . In the current study, we adopt a local measurement approach for elastic properties using nanoindentation, focusing specifically on the value of Young's modulus. Based on the investigations of Felten et al. [3] and Sadowski and Nowicki [13], Poisson's ratio is assumed to be  $\nu = 0.26$ , and this value is further validated by ultrasonics methods for the specified material.

The Nano-Hardness Tester (NHT) is equipped with an active reference featuring a capacitive force sensor. The NHT device employed enables the addition of an oscillating force with a low amplitude to measure contact stiffness during experiments. This method, defined by Oliver and Pharr [14], is known as the continuous stiffness measurements method. For the various tests presented in this study, a Berkovich's tip is utilized.

A network of 12 nanoindentation tests is randomly conducted on a polished specimen to gather statistical data regarding the material behavior attributed to the composition of the material (WC and Co phases). Nanoindentation tests are carried out with a progressively increasing and alternating applied force. This loading approach enables the acquisition of more than thirty loading/unloading cycles with different force levels for each nanoindentation test. The loading phases result in elastic-plastic responses, while the unloading phases exhibit elastic responses. Throughout each test, the nanoindentation force vs. indenter displacement curve is recorded.

From the unloading part, the unloading slope, denoted  $S$  is calculated. According to studies by Oliver and Pharr [14,15], the reduced elastic modulus  $E^*$  is related to the slope  $S$  and the projected contact surface area under the indenter  $A$  by the following expression:

$$E^* = \frac{\sqrt{\pi}}{2\beta} \frac{S}{\sqrt{A}} \quad (3)$$

The reduced elastic modulus  $E^*$  is also related to the elastic properties of the indenter ( $E_i, \nu_i$ ), and the indented material ( $E, \nu$ ) as follows:

$$\frac{1}{E^*} = \frac{1 - \nu_i^2}{E_i} + \frac{1 - \nu}{E} \quad (4)$$

The coefficient  $\beta$  is dependent on the indenter geometry, and in our case,  $\beta = 1.034$ . From force-displacement curves, the evolution of the reduced elastic modulus  $E^*$  is obtained as a function of the penetration depth  $h$ . For the UNH tester under consideration, the elastic properties of the diamond indenter are  $E_i = 1141 \text{ GPa}$  and  $\nu_i = 0.07$ .

### 2.3. Toughness determination at meso-scale from micro-indentation tests

Toughness at the meso-scale can be assessed by conducting Vickers tests under high loads. Indentations are performed on  $230 \mu\text{m}$  thick,  $30 \text{ mm}$  diameter disks. These disks are obtained through wire electrical discharge machining, and the plane surface quality is enhanced by a grinding process. To apply the desired loading, a Wolpert's micro-indentation apparatus is utilized with a Vickers tip.

Cracks become observable at a loading of  $10 \text{ N}$ , but it is insufficient for measuring crack lengths with a high level of repeatability. To ensure

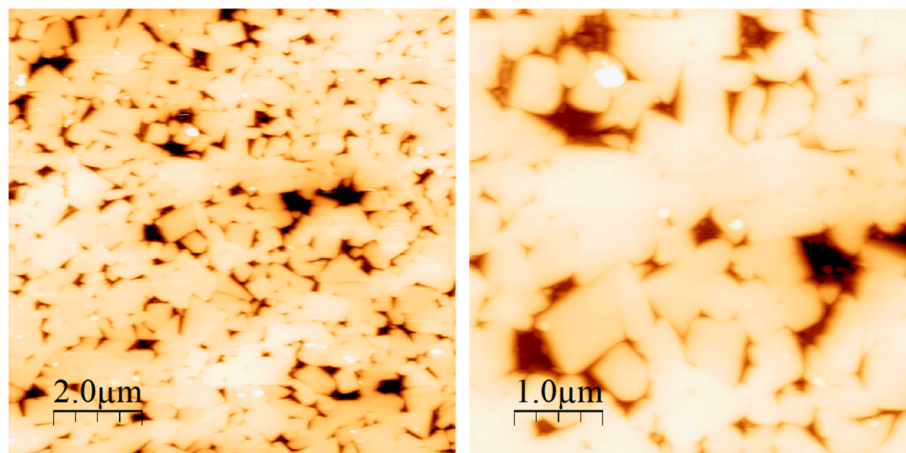


Fig. 2. WC-Co cemented carbide microstructure observed by Atomic Force Microscopy (average grain size =  $0.6 \mu\text{m}$ ).

measurements with an optical microscope, microindentation tests are performed under a 98 N loading. A network of 15 imprints has been created under this specified loading, with a 2 mm distance between each imprint to avoid any influence from the previous imprint.

To characterize hardness and toughness properties, it is essential to determine crack lengths  $l_i$  at each imprint corner and the two-imprint diagonals  $d_i$  (see Fig. 3b).

In the case of cemented carbide with a cobalt matrix, crack propagation mode is associated with radial or Palmqvist's mode [8]. The hardness value  $H$  is then defined by

$$H = \frac{P}{2\bar{d}} \quad (5)$$

where  $P$  is the applied loading and  $\bar{d}$  is the average semi-diagonal length defined by

$$\bar{d} = \frac{d_1 + d_2}{4} \quad (6)$$

The imprint diagonals and cracked lengths have been measured using an optical microscope with magnification ranging from 50× to 100×. Imprints and the associated cracks are shown in Fig. 3 a. In the case of Palmqvist's crack, the toughness value is reduced to mode I, and the critical stress intensity factor is denoted as  $K_C = K_I$ . This factor is linked to the hardness value  $H$ , the applied loading  $P$  and cracks lengths  $l_i$ .

Shetty et al. [9] proposed the following relation to extract the value of stress intensity factor in relation to  $H$ :

$$K_I = 0.0319\sqrt{HW} \quad (7)$$

where

$$W = \frac{P}{\sum_{i=1}^4 l_i} \quad (8)$$

This relation is also utilized by the International Organization for Standardization as presented by Swab and Wright [11], and defined as the ISO 28079 standard method.

Niihara et [7]. introduced a modification of this relation and proposed different model in relation with the  $\frac{l_i}{a}$ -ratio. The proposed models incorporate the effect of material stiffness through Young's modulus. In

our case  $0.25 \leq \frac{l_i}{a} \leq 2.5$ , the stress intensity factor is then given by:

$$K_I = 0.0246 \left( \frac{E}{H} \right)^{\frac{3}{8}} \sqrt{HW} \quad (9)$$

From these relations and the measurements of  $W$  and  $H$ , it is then possible to calculate the stress intensity factor.

#### 2.4. Toughness determination at micro-scale from micro-bending tests

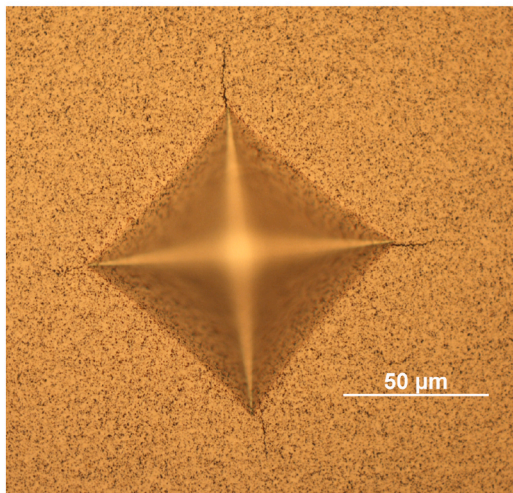
##### 2.4.1. Bending tests on micro-beams

To characterize the toughness behavior of WC-Co cemented carbide material at the micro-scale, bending tests on fix-free pre-cracked microcantilevers with three different loading cases are proposed. The initial micro-beam geometries are defined in Fig. 4.

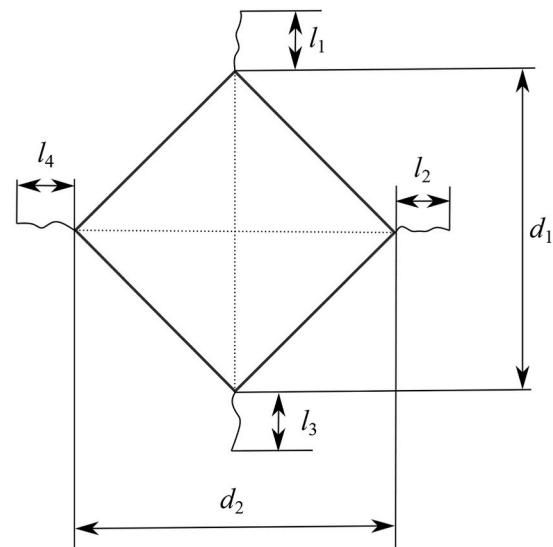
Micro-beams are obtained by using different micromanufacturing processes. Initially, a 250 μm thick disk is fabricated through wire electrical discharge machining and a grinding process to calibrate the disk thickness and ensure that the two opposite faces are parallel. This parallelism is crucial for the repeatability of the micro-bending test. In the subsequent step, two micro-electrical discharge machining (micro-milling) processes are performed with a calibrated rod electrode. A 3900 × 12000 × 10 μm<sup>3</sup> (length × width × depth) rectangular pocket operation is conducted to define a support area for the nanoindentation reference annulus. It is also utilized to have a higher surface position than the beam thickness position to avoid any damage to the beam specimen during the calibration procedure. The second operation involves in a contouring operation to obtain precise, close to 1 μm tolerance, beam geometries. It results in specimens as presented in Fig. 5.

The third operation involves defining the pre-cracked geometries for each beam at a fixed position nearest the bottom of the beam. For this, a focus ion beam (FIB) process is utilized with a z-sweep operation, in the transverse beam direction, located at a position of 300 μm from the bottom of the beam (Fig. 6).

This approach has also been utilized by Brinckmann et al. [16] and, in particular, by Bohnert et al. [5] to fabricate the complete geometry of monocrystalline tungsten beams. Platinum plating and surface preparation by FIB have also been tested to create, at the indenter application point, a local surface area for a repeatable point in each test. However, after testing, the results indicate that this preparation is not necessary for achieving repeatable tests.



a.



b.

Fig. 3. Imprint definition in microhardness test configuration: a) Imprint, b) Cracks dimensions.

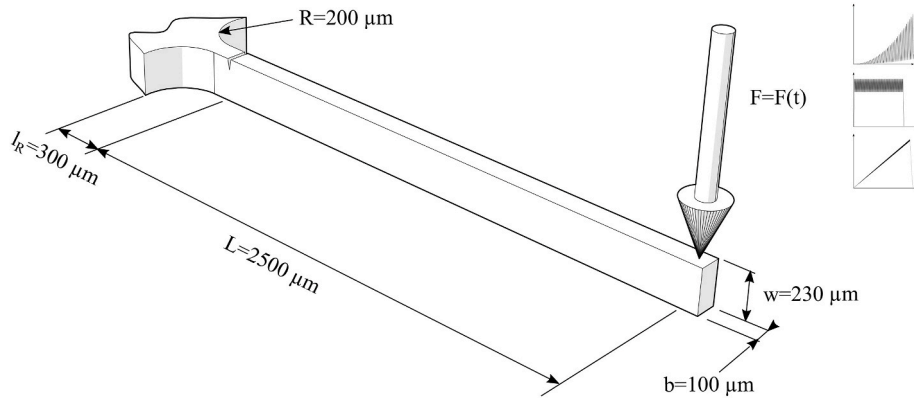


Fig. 4. Definition of the micro-cantilever's geometry.

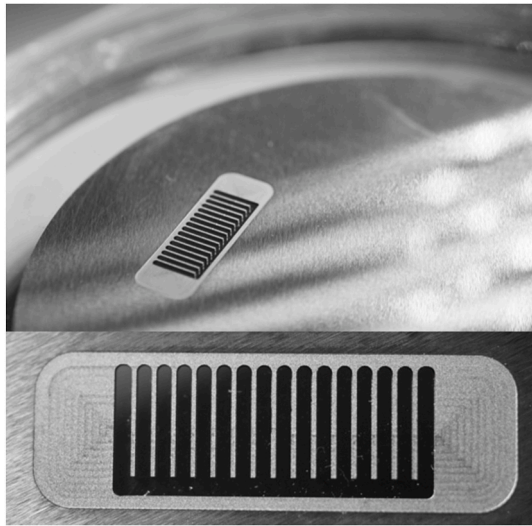


Fig. 5. Micro-beams network after micro-electrical discharge machining and grinding process.

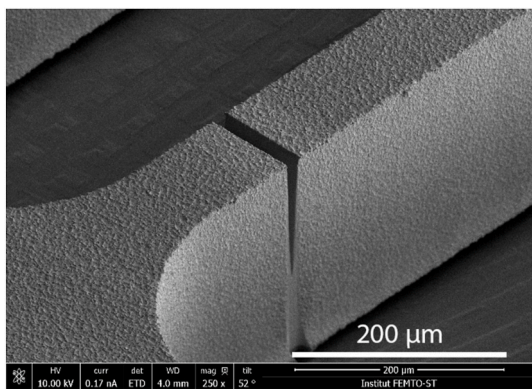


Fig. 6. Pre-cracked geometry obtained by Focus Ion Beam process.

According to Volkert and Minor [17], the FIB process only produces structural modifications to a maximum depth of around 20 nm. Based on this result, nanocracks at microcrack tip are very limited and have no significant influence on toughness properties at the micro-scale.

To ensure adequate loading force, the NHT indentation device is used. Three different loading conditions have been tested: progressive repeated loading (PRL), fatigue, and a ramping-sinus loading. These loadings are presented in Fig. 7.

In the first instance, a progressive repeated loading was tested. It consists of applying a cyclic triangular shape with a quadratic evolution of the maximum applied force at the end of each cycle (Fig. 7a). This type of loading is used to determinate the range of the critical fracture force noted  $F_c$ . By considering, a Fourier series representation of a triangular periodic function  $\varphi_\Lambda$ , with a natural frequency  $f$ , as:

$$\varphi_\Lambda(t) = \frac{8}{\pi^2} \sum_{k=0}^{\infty} \frac{(-1)^k}{(2k+1)^2} \sin(2(2k+1)\pi ft) \quad (10)$$

It then leads to the following mathematical expression of progressive repeated loading:

$$F_{prl}(t) = a_1 t^2 + b_1 + \frac{F_{sat}}{2} (1 + \varphi_\Lambda(t)) \left(\frac{t}{t_\infty}\right)^2 \quad (11)$$

The second approach is based a fatigue-like loading and consists of applying a triangular periodic loading with a non-zero mean loading value  $F_{mean}$  between two extreme values  $F_{max}$  and  $F_{min}$  (Fig. 7b). From the mathematical point of view, it can be expressed as:

$$F_{fig}(t) = \frac{F_{max} + F_{min}}{2} + \frac{F_{max} - F_{min}}{2} \sin(\pi ft) \quad (12)$$

$F_{min}$  and  $F_{max}$  are the minimum and maximum applied forces, respectively, and this loading is applied over  $n$  cycles.

Finally, a ramping sinus loading is proposed. It is defined as the superposition of a ramping loading (a linear progressive loading) and a sinus loading with a progressive increasing amplitude (Fig. 7c). From the mathematical point of view, the loading force  $F_{rsl}$  is linked to time  $t$  by the following equation:

$$F_{rsl}(t) = a_1 t + A_\infty t \sin(2\pi ft) \quad (13)$$

where  $a_1$  is the slope of the linear loading,  $A_\infty$  and  $f$  are the amplitude rate and the frequency of the periodic loading, respectively. Parameters values for each type of considered loading are reported in Table 1.

#### 2.4.2. Numerical determination of stress intensity factor

Bending tests lead to determining the critical fracture force  $F_c$  in order to identify the critical stress intensity factor. A finite element model is then proposed to build the numerical response and compared to experimental results to relate stress intensity factor  $K_I$  and the applied force  $F$  using the crack tip displacement field. 2D plane strain models are used to correlate numerical and experimental responses. The geometrical model and the associated mesh are presented in Fig. 8.

The 2D geometry is defined by a rectangular shape (A-B-C-D vertices). The pre-cracked geometry is classically defined by two initially overlapping lips between the points  $N_1$  and I, and  $N_2$  and I respectively. On each lip, two reference points are defined (M and L on left lip, K and J on right lip respectively) to determine numerically stress intensity factors. The point I corresponds to the crack tip. The ANSYS

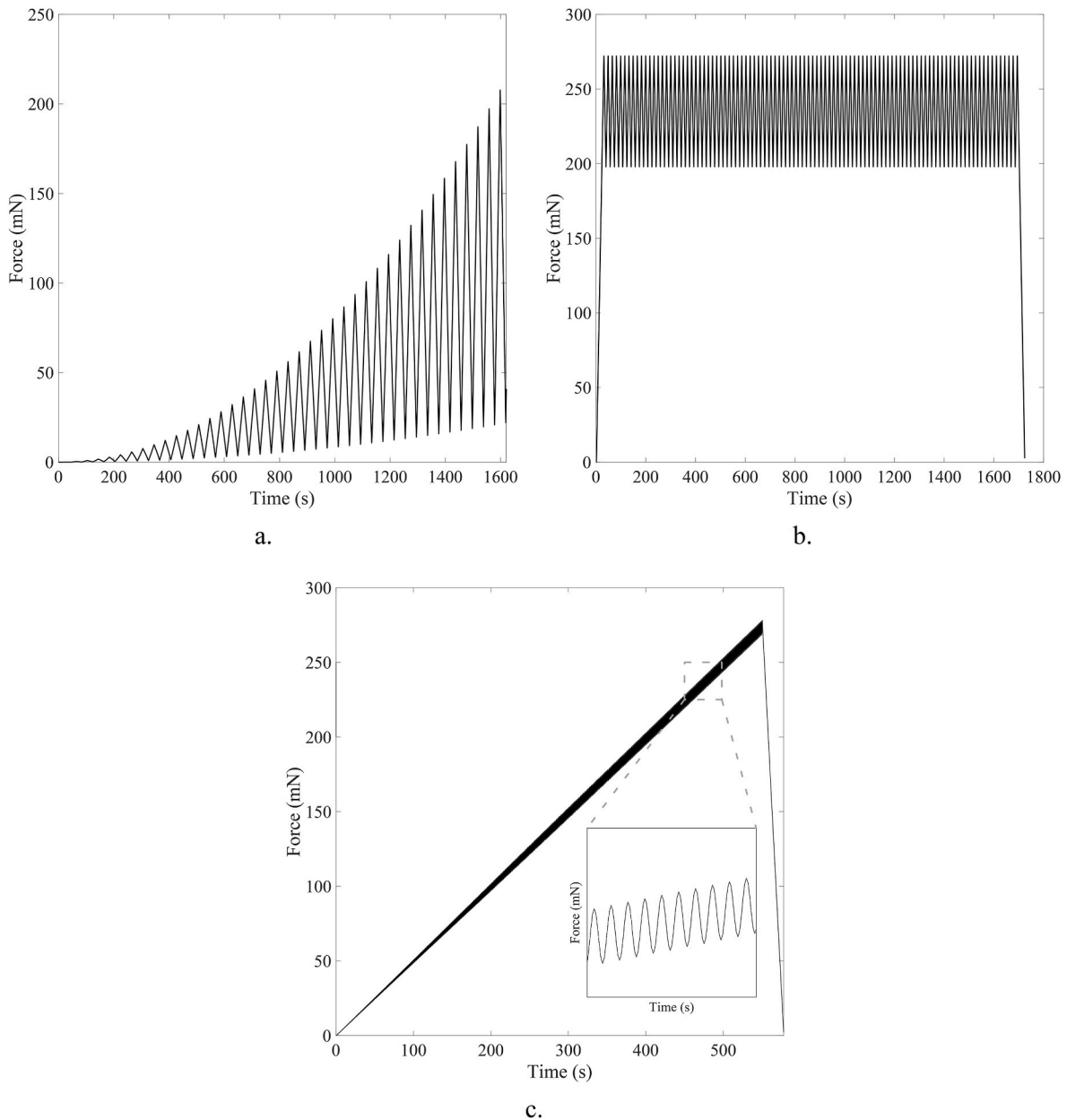


Fig. 7. Micro-beam loading cases: a. Progressive Repeated Loading, b. Fatigue-like loading, c. Ramping sinus loading.

Table 1

Parameters values associated to the different applied loadings.

Progressive Repeated Loading				
$\alpha_1$ (mN.s <sup>-2</sup> )	$b_1$ (mN)	$f$ (mHz)	$F_{sat}$ (mN)	$t_{\infty}$ (s)
$8 \times 10^{-6}$	0	25	46	790
Fatigue-like loading				
$F_{min}$ (mN)	$F_{max}$ (mN)	$f$ (mHz)	–	–
198	272	60	–	–
Ramping Sinus Loading				
$\alpha_2$ (mN.s <sup>-1</sup> )	$A_{\infty}$ (mN.s <sup>-1</sup> )	$f$ (mHz)	–	–
0.5	$10^{-2}$	1	–	–

Finite element code is used and eight nodes quads elements (QUAD183) are considered to improve precision and convergence rate. A linear and isotropic elastic model is used considering Young’s modulus and Poisson’s ratio obtained from nanoindentation as described in section 2.2. A convergence analysis was performed and a refined mesh is considered in the tip area (A-B-E-D area) as represented in Fig. 8 c. It leads to a mesh

with 23296 nodes and 7634 elements (Fig. 8c). In the tip area, the mesh is refined from a circular area centered at the tip location. To better capture the stress field singularity at the tip and determine stress intensity factor, a quarter point location technique, proposed by Barsoum [18], is used.

The A-B side is fixed ( $U_i = V_i = 0$  for each node on this side). The experimental fracture force  $F_{\infty}$  is applied at G-point.

From the displacement of M, K, L, J points, it is then possible to determine stress intensity factors ( $K_I, K_{II}, K_{III}$ ). Due to the 2D plane stress assumption, the  $K_{III}$  has a zero value. In principle, bending tests need to determine the value of  $K_{II}$  (shear stress) but the beam geometry ( $L \gg w$ ) allows neglecting this stress intensity factor. Therefore, it leads to determine the unique stress intensity factor  $K_I$ . By considering Fig. 8 d, the  $K_I$ -stress intensity factor is numerically determined, assuming plane stress assumption, by:

$$K_I = \lim_{r \rightarrow 0} \sqrt{2\pi} \frac{E}{8(1-\nu^2)} \frac{|\Delta d|}{\sqrt{r}} \tag{14}$$

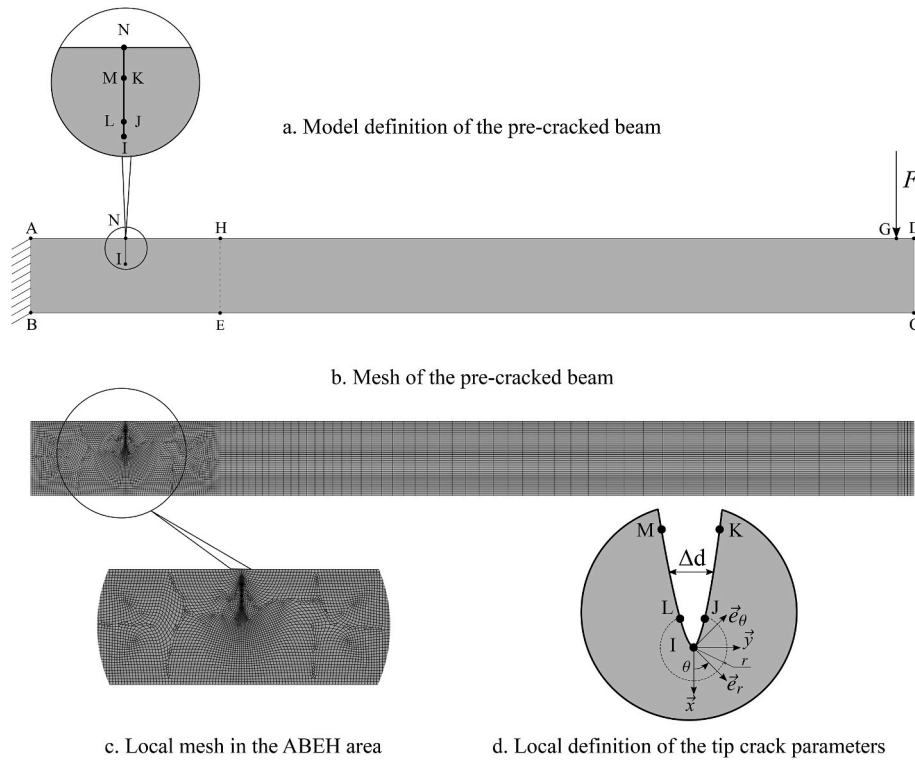


Fig. 8. Finite element model of the pre-cracked beam: a. Model definition, b. Mesh, c. Local definition of the mesh in tip area, d. Tip crack parameters.

where  $d$  is the transverse displacement in the  $\vec{y}$ -direction (local basis defined at the crack extremity in Fig. 8) and  $\Delta d$  is the relative displacement between two couples of points in the crack (M,K and L,J respectively). A local cylindrical basis  $(\vec{e}_r, \vec{e}_\theta)$  is also defined at point I. In this local basis,  $r$  is associated to the current radius relatively to the point and oriented by  $\theta$  angle. When  $r \rightarrow 0$ , it is considered that:

$$\frac{|\Delta d|}{\sqrt{r}} = A + Br \tag{15}$$

The  $A$  and  $B$  parameters are determined by measuring the displacement between the two couples of points (M, K) and (L, J) respectively in the crack for their associated positions  $(r, \theta)$  in the local cylindrical basis  $(\vec{e}_r, \vec{e}_\theta)$ . Finally, at the crack extremity, i.e.  $r \rightarrow 0$ , the stress intensity factor  $K_I$  value is defined by:

$$K_I = \sqrt{2\pi} \frac{E}{8(1-\nu^2)} A \tag{16}$$

Gross and Srawley [19] and Murakami [20] have proposed analytical formulae and tables to evaluate stress intensity factor from different classical tests as a function of the initial crack length  $a$ . By considering equation (1), the correction function  $f(\alpha)$  is given by:

$$f(\alpha) = 1.122 - 1.14\alpha + 7.33\alpha^2 - 13.08\alpha^3 + 14\alpha^4 \tag{17}$$

To compare this empirical approach with the proposed finite element model, the numerical model is parameterized to change the initial crack length  $a$  while keeping the beam width  $w$  constant. Eleven simulations are performed by varying the  $\alpha$ -ratio from 0.1 to 0.6 with a 0.05 increment. This approach is used to validate that the assumption of a stress state in the micro-beam is closed to pure bending and that the second stress intensity factor  $K_{II}$  can be neglected.

### 3. Results and discussion

#### 3.1. Determination of the elastic properties by nanoindentation

The identification of Young’s modulus is performed by nanoindentation tests. These results show a great variability of the Young’s modulus for low penetration values (under 300 nm). Over 300 nm, the Young’s modulus value is quite constant and repeatable. It is justified by the influence of the WC-Co cemented carbide microstructure and also the shape calibration of the indenter. The indentations are large enough to obtain an average response of the material. The maximum indentation depth is 900 nm. Knowing the geometry of the indenter, the plasticized zone at the surface of the sample is about 6  $\mu\text{m}$  large. It is sufficient to obtain an average response of the material, at least elastically.

In this range, a mean - value of the Young’s modulus equal to  $E = 654 \pm 50$  GPa is considered. Nevertheless, an analysis of the nanoindentation imprint from Atomic Force Microscopy shows that pile-up effect appears. It leads to an underestimated projected contact surface area  $A$  on the order of 12.5%. The value of the Young’s modulus is then corrected to  $E = 582 \pm 50$  GPa and the Poisson’s ratio is considered equal to  $\nu = 0.26$ . These results are in agreement with the values presented by Felten et al. [3].

#### 3.2. Toughness determination from micro-indentation tests

Vickers micro-hardness is applied to determine an initial reference for toughness properties in relation to the methods proposed by Shetty et al. [9], Swab and Wright [11] and Niihara et al. [7]. The applied penetration force is equal to 98 N. From Fig. 3 a, it can be observed that there are four cracks on each vertex. As expected and defined by Warren and Matzke [8], WC-Co cemented carbide exhibits radial or Palmqvist cracks. In relation to the homogeneous structure of the cemented carbide studied, at the scale of the test, the determination of the lengths of the imprint diagonals is very repeatable with a value equal to  $d_i = 107.6 \mu\text{m}$  with a standard deviation value equal to  $SD(d_i) = 0.986 \mu\text{m}$ . On the contrary, the measurement of crack lengths shows a great variability

**Table 2**  
Toughness values evaluation from Vickers microhardness measurements.

Method	Toughness value (MPa $\sqrt{m}$ )
Shetty [9]/ISO 28079 [11]	13.81 $\pm$ 4.05
Niihara [7]	15.72 $\pm$ 5.65

with a mean value  $l_i = 17.5 \mu\text{m}$  with a standard deviation value equal to SD ( $l_i$ ) = 4.58  $\mu\text{m}$ . In this context, the uncertainty of measurement is close to 30% for the ISO 28079 method and to 35.7% with the Niihara's method respectively. Toughness values are reported in Table 2.

These results are close to the values proposed, for cemented-carbide material with a 10% cobalt matrix by Shetty et al. [9] and Swab and Wright [11]. It shows the difficulty of obtaining an accurate value of the critical stress intensity factor from these methods. As in the case of micro-indentation tests leading to crack length measurements, the reliability of approximate analytical models is open to criticism. The determination of the critical stress intensity factor is then an approximation of an equivalent model and depends on accurate measurement of the cumulated crack length. This leads to cumulating measurement errors and approximation errors of the models used.

### 3.3. Determination of the critical fracture force

From the instrumented nanoindentation method with the three types of loading (Progressive repeated, fatigue-like and ramping sinus loadings), the critical fracture force  $F_c$  is determined. Progressive Repeated and fatigue-like loadings are used to evaluate the range of the critical fracture force. Ramping sinus loading are then applied to determine precisely the critical fracture force value. These first two types of loading used are rather conventional but have a number of drawbacks. Progressive Repetitive Loading enables the load to be ramped up, but rapid loading and unloading create singularities that can lead to failure at lower loads. In the case of fatigue loading, it is not easy to determine the stress range. If the load or the loading rate are too high, failure may occur during the first load increase. In the case of fatigue loading, superimposing a periodic loading, equivalent to the ramping sinus loading case, could also be an interesting solution but has not yet been tested.

Three beams are used for each loading to ensure test repeatability, and the force/displacement curves during micro-bending tests are presented in Fig. 9. As mentioned previously, the progressive repeated and fatigue-like loadings were used to determine the critical force measurement range, defined in the range  $F_c = [230 \text{ mN}; 300 \text{ mN}]$ .

By using the results from ramping sinus loading (Fig. 9c), it can be observed that the determination of the critical force is very repeatable in a displacement range of 36  $\mu\text{m}$  and 38  $\mu\text{m}$ . In our case, the ramping sinus loading leads to determine a critical force  $F_c = 290 \pm 2 \text{ mN}$ .

It is also possible to determine the critical force with accuracy by considering the phase shifting between the applied force and the induced indenter displacement, as represented in Fig. 10.

At the beginning of the loading, contact research is observed with a significant variation between the applied force and the resulting displacement. When permanent contact is obtained, the time shifting is constant and equal to  $t_s = 0.01 \text{ s}$  due to the machine servo control response. When a crack is initiated, fracture leads to a loss of rigidity and a delay is observed between the applied (control) force and the indenter displacement, allowing for the accurate determination of the instant when the crack propagates. In this case, it is observed that crack initiation appears for a tip displacement in the range of 26  $\mu\text{m}$ –28  $\mu\text{m}$ . This corresponds to a slight deviation from the linear fit of the force/displacement curve, which is difficult to detect directly. It leads to determining a lower value of the critical force  $F_c = 240 \pm 2 \mu\text{N}$  and, therefore, a lower critical stress intensity factor value. In relation to Fig. 10, a repeatable process in terms of phase shift response can be

observed. By considering the study of Felten et al. [3], a slight deviation from the linear fit is also demonstrated on the resistance curve (R-curve) for a WC-Co cemented carbide. The fracture toughness is determined in the plateau region (constant value) of the R-curve. In principle, the time-shifting curve has to be considered to identify the critical force. To compare our results with the classical approach, the critical force determined on the displacement/force curve (Fig. 9c) with the ramping sinus loading is initially used. However, the stress intensity factor value will also be calculated with the critical force in the case of time-shifting observation.

### 3.4. Numerical determination of the critical stress intensity factor

The numerical model is then used to determine the critical stress intensity factor by considering the critical fracture force  $F_c$  obtained from bending tests with the ramping sinus loading. This value is used and applied at the G-point, as presented previously. The equivalent stress field (von Mises) is presented in Fig. 11. This field is then concentrated in the crack tip area as expected to determine critical stress intensity factor.

By considering the numerical methodology, the stress intensity factor is extracted. The model is compared with analytical models proposed by Gross and Srawley [19] and Murakami [20]. In relation to equation (1), the evolution of stress intensity factor as a function of the  $\alpha$ -parameter is presented in Fig. 12.

The numerical response for a fix-free beam with an applied transverse force is close to Murakami's model related to a fix-free beam under pure bending. It confirms that the assumption of a fix-free beam is correct for this configuration. The Bohnert's model slightly underestimates the stress intensity factor, but the authors attribute this offset to the use of a non-standard geometry beam. However, it is important to mention that this offset is weak and leads to a relative error between the two methods of less than 6%. These comparisons allow us to validate the 2D model approach and the assumption based on an equivalent pure bending loading. Due to the FIB process, the initial crack is not a closed one and induces a not perfectly 2D geometry (Fig. 6). A second numerical model has been tested by considering an initial open crack with a positive opening. The geometrical default due to the FIB process is a V-notched crack geometry and leads to non-overlapping lips in the pre-cracked beam. It has been shown that this consideration has no influence on the determination of stress intensity factor. Thus, a pre-cracked geometry with two overlapping lips is appropriate in relation to the initial crack length  $l_1$ . In the case of the considered beam, the FIB process induces a slight variation in the notched geometry, as represented in Fig. 13.

On the edge of the crack, the manufacturing process leads to a longer length than the beam width. In relation to the study of Brinckmann et al. [16], this defect has minimal influence on the determination of the stress intensity factor (less than 10%), and the crack length has to be considered in the mid-width of the specimen. A 3D numerical simulation also supports this assumption. It leads to considering an initial crack length  $l_1 = 52 \mu\text{m}$ .

By using the numerical simulation and varying the value of each parameter within the uncertainties interval, the stress intensity factor has been obtained and gives  $K_{Ic} = 10.43 \pm 0.69 \text{ MPa } \sqrt{m}$ . The mean value is lower than the values obtained by micro-indentation with the ISO 28079 and Niihara's empirical models, with a lower uncertainty range. Nevertheless, this value is very close to the value obtained by four-point bending test on a cemented-carbide with a 10% cobalt matrix, with a similar order of uncertainty in the study of Tarragó et al. [4]. In the case of 4-point bending test, prismatic bar of 45 mm  $\times$  4 mm  $\times$  3 mm dimensions are considered, which is approximately 20 times longer and thicker than the micro-beams considered for the micro-bending tests. It seems that the miniaturization does not influence toughness properties in this case (no scale effect). Comparisons between the micro-bending tests with ISO 28079 and Niihara's methods are summarized in Table 3.

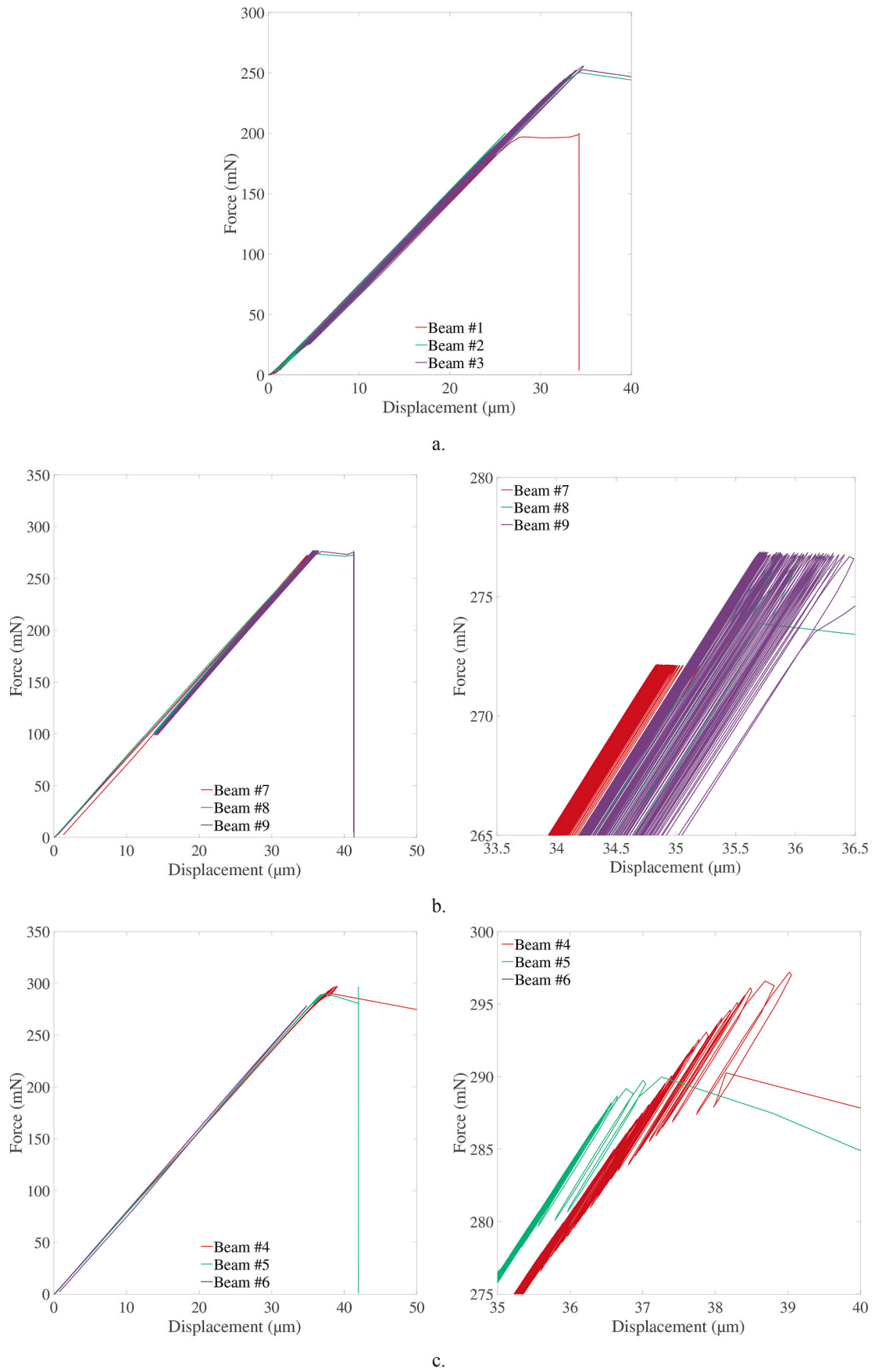


Fig. 9. Applied force/resulting displacement curves for different types of loading: a. Progressive repeated loading, b. Fatigue-like loading, c. Ramping sinus loading.

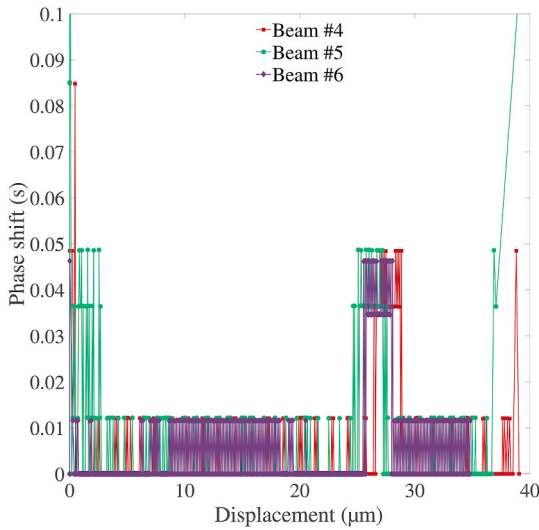


Fig. 10. Time shifting between applied force and resulting displacement.

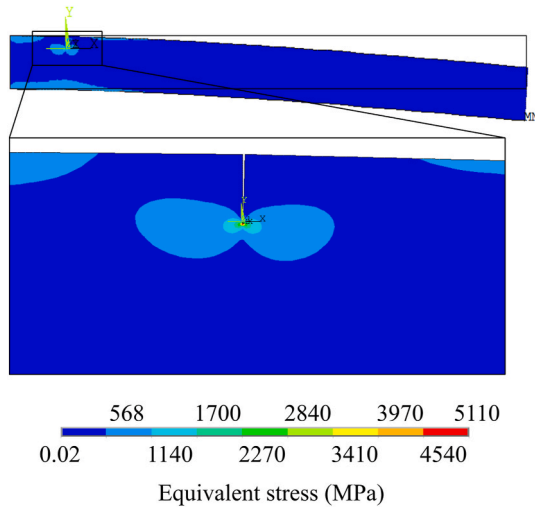


Fig. 11. Equivalent (von Mises) stress field in the specimen and in the crack tip area (Maximum value = 5110 MPa).

Comparison with the results obtained by Felten et al. [3] from CT tests is also proposed. They demonstrated that the critical stress intensity, for WC-Co materials, is dependent on the volume binder content  $V_{Co}$  (volume fraction of Cobalt phase). For a cemented carbide with a volume binder content of  $V_{Co} = 12.5\%$ , the critical stress intensity factor is  $K_{Ic} = 12.6 \text{ MPa} \sqrt{m}$ . In the case of a pure tungsten carbide material ( $V_{Co}=0\%$ ), the critical stress intensity factor is evaluated to  $K_{Ic} = 6 \text{ MPa} \sqrt{m}$ . In first approximation, with a linear interpolation, it can be considered for a volume binder content  $V_{Co} = 10\%$  that the value of the fracture toughness is equal to  $K_{Ic} = 11.28 \text{ MPa} \sqrt{m}$ . By considering the determination of critical force, equal to  $F_c = 240 \pm 2 \text{ mN}$ , from the time shifting evolution, the critical stress intensity factor is  $K_{Ic} = 8.63 \text{ MPa} \sqrt{m}$ . In comparison with the evolution of the R-Curve proposed by Felten et al. [3], it can be found that the value is  $K_{Ic} = 9.13 \text{ MPa} \sqrt{m}$  and it is close to the results presented in this paper.

It comes that the instrumented micro-bending test, using a nano-indentation apparatus with ramping sinus loading, is very accurate and repeatable to determine the critical fracture force, at the micro scale. In the same manner, specimen fabrication and preparation from EDM to FIB process are also very repeatable. A less than  $1 \mu\text{m}$  thick heat-affected zone has been measured, leading to limit any initial pre-cracked at the

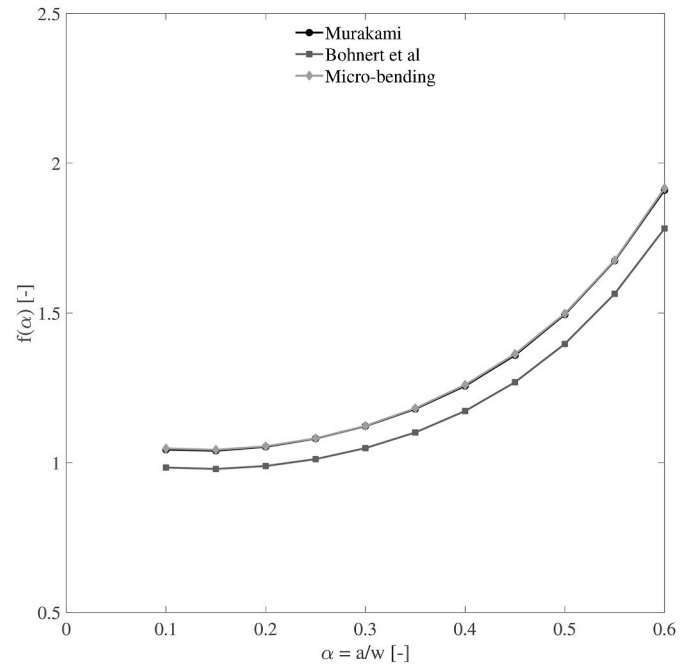


Fig. 12. Comparison of the evolution of  $f(\alpha)$  for different initial crack length ratio  $a/w$  between the proposed model and analytical models.

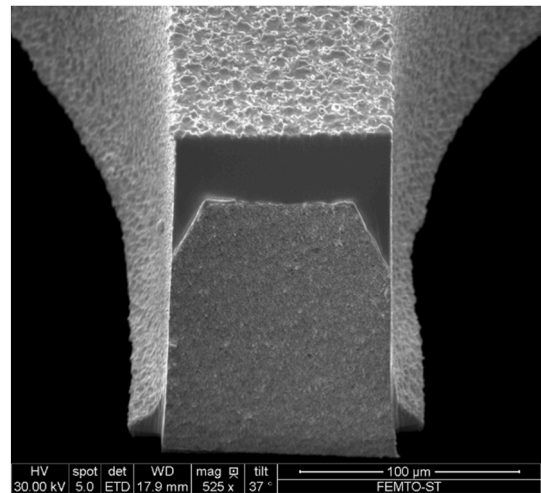


Fig. 13. Pre-cracked geometry observed after fracture.

Table 3

Critical stress intensity factor values from micro-hardness methods and the proposed micro-bending (MB) tests.

Critical stress intensity factor $K_{Ic}$ (MPa $\sqrt{m}$ )				
ISO 28079 [9,11]	Niihara [7]	4-point bending test [4]	MB (Force vs Disp.)	MB (Time Shift)
$13.81 \pm 4.05$	$15.72 \pm 5.65$	$10.4 \pm 0.3$	$10.43 \pm 0.69$	$8.63 \pm 0.69$

specimen surface. The thickness of the heat-affected zone is less than  $1 \mu\text{m}$  and does not introduce a pre-crack. All the assumptions made from micro-hardness tests lead to pile-up experimental errors and model approximation.

#### 4. Conclusions

The aim of this study was to investigate the development of micro-bending tests, from an nanoindentation device, coupled with a finite element model to determine toughness properties, at micro-scale, of a WC-Co cemented carbide. Based on the presented results, the following conclusions may be summarized:

- Instrumented Micro-Bending Test with ramping sinus loading:** The use of a nanoindentation device with ramping sinus loading provides an accurate and repeatable method for determining the critical fracture force at the micro-scale. The specimen fabrication, preparation, and loading procedures contribute to the repeatability of the tests.
- Specimen Fabrication and Preparation:** The fabrication and preparation of specimens, from electrical discharge machining (EDM) to focus ion beam (FIB) processes, are highly repeatable. A minimal heat-affected zone has been measured, limiting the introduction of pre-cracks at the specimen surface.
- Finite element model:** The 2D finite element model used for stress intensity factor determination in micro-bending tests is validated by comparing it with analytical models. The assumption of a fix-free beam and consideration of an initial crack length in the mid-width of the specimen are found to be appropriate.
- Comparison with previous studies:** The critical stress intensity factor  $K_{Ic}$  obtained from micro-bending tests is comparable to values reported in the literature for cemented carbide materials. Comparison with results from CT tests Felten et al. [3] and 4-point bending test at macro-scale by very closed to the result obtained on an equivalent material with 4-point bending test at macro-scale by Tarragó et al. [4] supports the accuracy and reliability of the developed micro-bending test.
- Challenges in Toughness characterization:** Challenges exist in accurately characterizing toughness properties, especially when using empirical models based on micro-indentation tests. The reliability of such models depends on precise measurements of crack lengths, introducing high uncertainties.
- Scale Effect:** The miniaturization of the micro-bending test does not seem to introduce significant scale effects in determining toughness properties, as evidenced by results comparable to those obtained from larger-scale bending tests.
- Future considerations:** While the presented micro-bending test provides valuable insights, further investigations and refinements in experimental and numerical methodologies could enhance accuracy and broaden of the method. Firstly, extending the method to other harder and more brittle materials (ceramics) is essential. The adaptation to such materials must also involve investigating optimal loading conditions. The superposition of a periodic signal onto fatigue loading is worth exploring in addition to ramping sinusoidal tests. The method developed here can be applied to materials with higher capacities, for example by adjusting the length of the beams. The proposed method is also highly dependent, as is every method, on the sample manufacturing process. In the case of EDM processes, conductivity of the material is a crucial property. The FIB process is an alternative for ceramic materials, but requires a very long manufacturing time and is limited in terms of sample dimensions. Another process to be consider is femto-second laser beam processes but a specific study on the influence of local geometry could be necessary.

The proposed method, which involves ramp loading with superimposed periodic loading, has proven to be effective. It would be interesting to explore the efficacy of incorporating this periodic loading

in other scenarios, especially in fatigue-like cases. This represents the primary focus of future work to determine critical loads more efficiently. These conclusions underscore the potential of the developed micro-bending test as a reliable and repeatable approach for toughness characterization at the micro-scale. This contributes to the understanding of material behavior in WC-Co cemented carbides and, by extension, other materials with high fracture toughness, such as ceramics.

#### Credit author statement

**Julien Monnet:** Experimentation, numerical simulation, data analysis, writing-revision, **Martial Personeni:** Electrical Discharge machining, Experimentation, **Yves Gaillard:** Nanoindentation tests, experimentation, data analysis, reviewing **Fabrice Richard:** Nano-indentation tests, numerical modelling, data analysis, reviewing, **Sébastien Thibaud:** numerical simulation, data analysis, funding acquisition, supervision, Conceptualization, writing reviewing and editing.

#### Data availability

Data will be available on request.

#### Declaration of competing interest

The authors declare that they have no known competing financial interests or personal relationships that could have appeared to influence the work reported in this paper.

#### Acknowledgments

This work was financially supported by Université de Franche-Comté. Additionally, the authors acknowledge the MIFHySTO and AMETISTE facilities from FEMTO-ST Institute.

#### References

- Ingelstrom N, Nordberg H. The fracture toughness of cemented tungsten carbides. *Eng Fract Mech* 1974;6:597–607. [https://doi.org/10.1016/0013-7944\(74\)90016-2](https://doi.org/10.1016/0013-7944(74)90016-2).
- Fang ZZ. Correlation of transverse rupture strength of WC-Co with hardness. *Int J Refract Metals Hard Mater* 2005;23:119–27. <https://doi.org/10.1016/j.ijrmhm.2004.11.005>.
- Felten F, Schneider GA, Sadowski T. Estimation of R-curve in WC/Co cermet by CT test. *Int J Refract Metals Hard Mater* 2008;26:55–60. <https://doi.org/10.1016/j.ijrmhm.2007.01.005>.
- Tarragó J, Coureaux D, Torres Y, Casellas D, Al-Dawery I, Schneider L, Llanes L. Microstructural effects on the r-curve behavior of wc-co cemented carbides. *Mater Des* 2016;97:492–501. <https://doi.org/10.1016/j.matdes.2016.02.115>.
- Bohnert C, Schmitt NJ, Weygand SM, Kraft O, Schwaiger R. Fracture toughness characterization of single-crystalline tungsten using notched micro-cantilever specimens. *Int J Plast* 2016;81:1–17. <https://doi.org/10.1016/j.ijplas.2016.01.014>.
- Pippan R, Wurster S, Kiener D. Fracture mechanics of micro samples: fundamental considerations. *Mater Des* 2018;159:252–67. <https://doi.org/10.1016/j.matdes.2018.09.004>.
- Niihara K, Morena R, Hasselman DPH. Evaluation of  $K_{Ic}$  of brittle solids by the indentation method with low crack-to-indent ratios. *J Mater Sci Lett* 1982;1:13–6. <https://doi.org/10.1007/BF00724706>.
- Warren R, Matzke H. *Indentation testing of a broad range of cemented carbides. In: Science of hard materials.* Springer; 1983. p. 563–82.
- Shetty DK, Wright IG, Mincer PN, Clauer AH. Indentation fracture of WC-Co cermets. *J Mater Sci* 1985;20:1873–82. <https://doi.org/10.1007/BF00555296>.
- Spiegler R, Schmauder S, Sigl LS. Fracture toughness evaluation of WC-Co alloys by indentation testing. *J Hard Mater* 1990;1:147–58.
- Swab JJ, Wright JC. Application of ASTM C1421 to WC-Co fracture toughness measurement. *Int J Refract Metals Hard Mater* 2016;58:8–13. <https://doi.org/10.1016/j.ijrmhm.2016.03.007>.
- Okamoto S, Nakazono Y, Otsuka K, Shimoiitani Y, Takada J. Mechanical properties of wc/co cemented carbide with larger wc grain size. *Mater Char* 2005;55:281–7. <https://doi.org/10.1016/j.matchar.2005.06.001>.

- [13] Sadowski T, Nowicki T. Numerical investigation of local mechanical properties of wc/co composite. *Comput Mater Sci* 2008;43:235–41. <https://doi.org/10.1016/j.commatsci.2007.07.030>. proceedings of the 16th International Workshop on Computational Mechanics of Materials.
- [14] Oliver WC, Pharr GM. Measurement of hardness and elastic modulus by instrumented indentation: advances in understanding and refinements to methodology. *J Mater Res* 2004;19:3–20. <https://doi.org/10.1557/jmr.2004.19.1.3>.
- [15] Oliver WC, Pharr GM. An improved technique for determining hardness and elastic modulus using load and displacement sensing indentation experiments. *J Mater Res* 1992;7:1564–83. Publisher: Cambridge University Press.
- [16] Brinckmann S, Matoy K, Kirchlechner C, Dehm G. On the influence of microcantilever pre-crack geometries on the apparent fracture toughness of brittle materials. *Acta Mater* 2017;136:281–7. Publisher: Elsevier.
- [17] Volkert CA, Minor AM. Focused ion beam microscopy and micromachining. *MRS Bull* 2007;32:389–99.
- [18] Barsoum RS. Further application of quadratic isoparametric finite elements to linear fracture mechanics of plate bending and general shells. *Int J Fract* 1975;11:167–9. <https://doi.org/10.1007/BF00034724>.
- [19] Gross B, Srawley JE. Stress-intensity factors for single-edge-notch specimens in bending or combined bending and tension by boundary collocation of a stress function. NATIONAL AERONAUTICS AND SPACE ADMINISTRATION CLEVELAND OH LEWIS RESEARCH CENTER; 1965. Technical Report.
- [20] Murakami Y. Stress intensity factors handbook. Pergamon; 1987.